Andrijana Đurđević[1], Srđan Tadić[2], Ivana Ivanović[2], Horia Dascau[3], Đorđe Đurđević[1]

NUMERICAL ANALYSIS OF HEAT TRANSFER DURING FRICTION STIR WELDING

NUMERIČKA ANALIZA PRENOSA TOPLOTE PRI ZAVARIVANJU TRENJEM SA MEŠANJEM

Originalni naučni rad / Original scientific paper
UDK /UDC: 621.791.1:536.2
Rad primljen / Paper received: 11.04.2017

Adresa autora / Author's address:
[1] Tehnikum Taurunum - College of Applied Engineering Studies, Belgrade, Serbia, email: andrijana.miler@yahoo.com
[2] University of Belgrade, Innovation Centre of the Faculty of Mechanical Engineering, Serbia
[3] ISIM, Timişoara, Romania

Keywords
- friction stir welding
- aluminium alloys
- numerical analysis
- temperature fields

Ključne reči
- zavarivanje trenjem sa mešanjem
- aluminijumske legure
- numerička analiza
- temperaturna polja

Abstract

The paper deals with the heat input and maximum temperature that develops in friction stir welding with different welding parameters. The finite element method has been used for numerical analysis of temperature distribution in a friction stir welded Al alloy. Results of temperature distribution in the friction stir welded T-joint and butt joint are presented.

Izvod

Razmatra se unos toplote tokom zavarivanja trenjem sa mešanjem, sa fokusom na maksimalnu vrednost temperature pri različitim parametrima zavarivanja. Metoda konačnih elemenata je primenjena na Al legure zavarene trenjem sa mešanjem. Prikazane su raspodele temperaturnih polja kod T-spoja i kod sučeonog spoja.

INTRODUCTION

Friction stir welding (FSW) is a recent method of welding in the solid state. In FSW, a cylindrical shouldered tool with a profiled probe, also called pin, is rotated and slowly plunged into the joint line between two pieces of sheet or plate material which are butted together, Fig. 1, /1/. The shoulder applies pressure to constrain the already deformed material around the probe tool. Positions of the FSW tool, working plates and welding direction are shown in Fig. 1.

In the friction stir welding process, heat is generated by friction between tool and workpiece. This heat flows into the workpiece as well as into the tool. The amount of heat conducted into the workpiece determines the quality of weld, residual stress, and distortion of the workpiece. The amount of the heat that flows into the tool dictates its life and capability for the joining process.

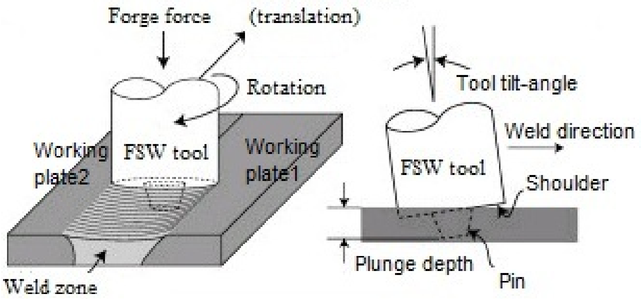

Figure 1. Simplified representation of FSW - butt joint.

In this paper the finite element method (FEM) is used to simulate temperature distribution in the workpiece. The discussion concerning the FSW process is given and is focused on differences in T- and butt joints. The results show that the majority of the heat generated from friction, i.e., about 95%, is transferred into the workpiece and only 5% flows into the tool and the fraction of the rate of plastic work dissipated as heat is about 80%, /2-4/.

NUMERICAL ANALYSIS

The modelling of the FSW welding process allows to visualize the fundamental behaviour of welded materials, and to study the influence of different welding parameters, including the design of the tool and boundary conditions, without performing costly experiments. The FSW modelling is a difficult task, because of its complex features. The process combines heat flow, high temperature, plastic deformation and microstructure evolution. Nowadays, the numerical simulation of the FSW process may not only be used to optimize the process. Increased knowledge produced based on the FSW process simulation can lead to replace experimental tests in the near future. This will help promote and expand the FSW process to a wider range of different applications.

Numerical simulations are made for the FSW process of two Al alloy working plates in order to obtain the T-joint (Fig. 2a) and butt joint (Fig. 2b). Two different FEM solvers were used, one for the T-joint (AA 5754) and another for the butt joint (AA 6061), /4/.

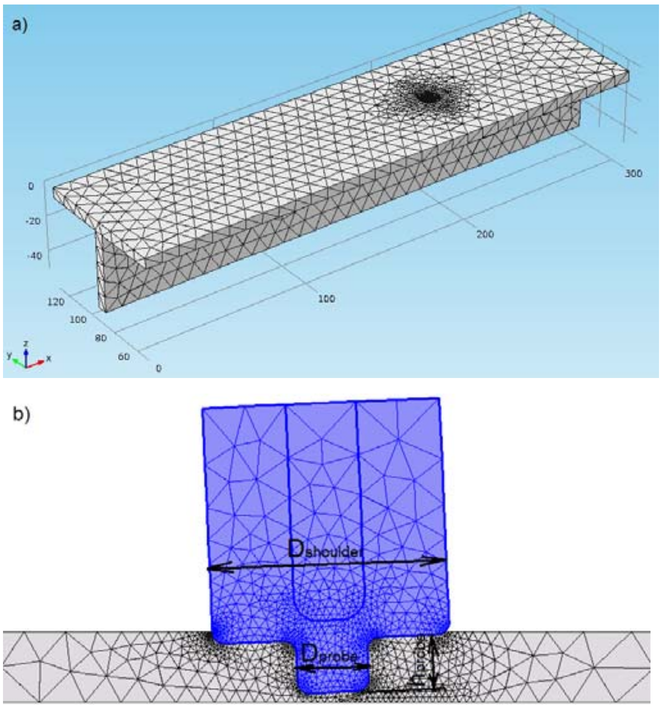

Figure 2. Mesh model of: a) T-joint and, b) butt joint.

Heat generation model

The heat transfer process is one of the most important aspects of the FSW study. A good understanding of the heat transfer process in the working plates can be helpful in predicting the thermal cycles, and the hardness in the welding zone, subsequently, can be helpful in evaluating the weld quality. Significant progress has recently been made of FSW heat transfer modelling, /4-8/.

In the FSW process, the heat is generated near the contact surfaces, which may have complex geometries depending on the tool shape. However, for the used model, the surface of the tool is assumed to be cylindrical with a horizontal shoulder. The welding tool is shown in Fig. 2b, where $r_{shoulder}$ is the shoulder radius, r_{probe} and h_{probe} are the probe radius and height, respectively.

The following assumptions are:

- heat generated at the shoulder of the welding tool/working plate interface is frictional heat,
- probe of welding tool is a cylinder, since the thread of the probe can be neglected,
- heat does not flow into the working plates if the local temperature reaches the material melting temperature.

The generated heat in the thermo-mechanical welding process occurs in two areas, Fig. 3, /9-11/:

1. Forehead of shoulder, i.e. the heat generated at shoulder of tool/working plate interface, where the size of the area of the top of shoulder is:

$$A_{shoulder} = \pi r_{shoulder}^2 \tag{1}$$

2. Around the tool probe, i.e. the heat generated at the probe of tool/plate interface, where the generated heat is modelled like a hole in the working plates, with area of probe given as:

$$A_{probe} = h_{probe} 2\pi r_{probe} + \pi r_{probe}^2 \tag{2}$$

The heat generated by the probe is estimated to be only 2% of the total heat generated during the FSW process. However, this ratio is estimated 20% by some researchers, /9-12/.

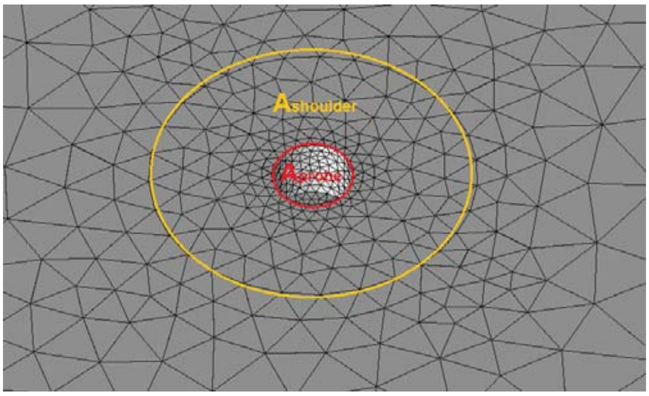

Figure 3. Two areas where the heat is generated in the welding process.

The total heat flux is split into the shoulder-flux (friction driven) and probe-flux (plasticity driven), /3/:

$$q = q_{shoulder} + q_{probe} = \\ = \mu \frac{F_n}{A_{shoulder}} r_{shoulder} v_{rot} + \frac{\mu \pi \sigma h_{probe} r_{probe}^2 v_{rot}}{\sqrt{3(1+\mu^2)}} \tag{3}$$

Actually, $q_{shoulder} = \mu \frac{F_n}{A_{shoulder}} r_{shoulder} v_{rot}$ is the heat generated by friction contact of surface forehead at the top of the shoulder and the upper surface of the working plate, /9/, where μ is the coefficient of friction, taken as constant here: $\mu = 0.3$. It was not possible to measure the pressure force, so its value is also taken as a constant, $F_n = 15$ kN. Finally, v_{rot} is the speed of rotation of the welding tool, also assumed to have a constant value, /8/. Heat generated by plastic deformation, q_{probe}, is modelled by using expression $\frac{\mu \pi \sigma h_{probe} r_{probe}^2 v_{rot}}{\sqrt{3(1+\mu^2)}}$, where σ (N/mm^2) is a yield stress of the working plate material.

As for the analysis of heat flow, numerical models can use either Eulerian formulation, Lagrangian formulation, or a combination of both (hybrid solution Lagrange-Eulerian). During the FSW process, the tool is moved with a constant speed along the joint line. The heat transfer control equation for the plates, in the case of Eulerian formulation with convection, can be written in following form, /8-9/:

$$\rho c \frac{\partial T}{dt} = \nabla(k \nabla T) + q - \rho c v_{wel} \nabla T \tag{4}$$

If the process is stationary, the first member in Eq.(4) is zero, i.e. $\rho c \frac{\partial T}{dt} = 0$. Thus, Eq.(4) is reduced to:

$$0 = \nabla(-k \nabla T) + \rho c v_{wel} \nabla T - q \tag{5}$$

Quantities used in Eqs.(4-5) are defined in Table 1.

Table 1. Quantities in Eqs.(4-5).

ρ (kg/m^3)	density
c (J/kgK)	heat capacity
T (K)	temperature
t (s)	time
$\nabla=\frac{\partial}{\partial x}+\frac{\partial}{\partial y}+\frac{\partial}{\partial z}$	differential operator
k (W/mK)	heat conductivity
q (W/m^2)	heat input
v_{wel} (m/s)	welding speed

Boundary conditions

Boundary and initial conditions for the T-joint are shown in Fig. 4, and for the butt joint in Fig. 5. Free surfaces are supposed to obey convection boundary conditions – upper surface exposed to room temperature air; the bottom surface is in a firm contact with the back plate of stainless steel type 304 for the T-joint, and L-316 for the butt joint. All materials and thermo dynamical parameters are used from literature data, typical for 5754 and 6061 aluminium alloys, /3/.

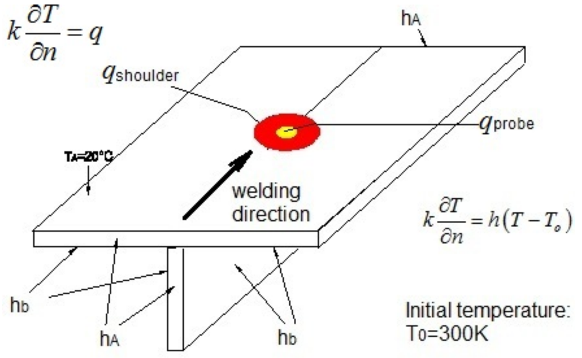

Figure 4. Boundary conditions for the T-joint.

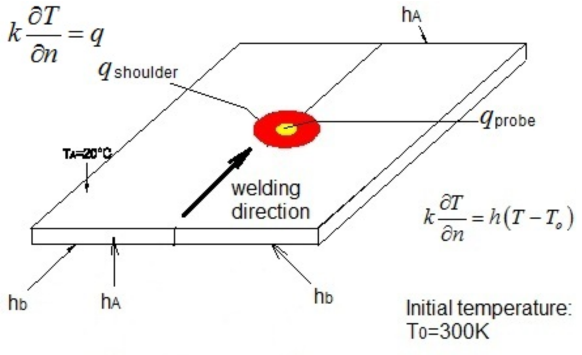

Figure 5. Boundary conditions for the butt joint.

Four boundary conditions are used. There are two convection boundary conditions, $k\frac{\partial T}{\partial n}=h(T-T_o)$, one for all plate surfaces exposed to air, and the second for all plate surfaces exposed to backing plates. The variable n is the normal direction vector of boundary on the surface of the plate; h is the coefficient heat convection from the plates to ambient air; and T_0 represents the temperature of ambient air.

The remaining two boundary conditions are: q_1 - the heat flux boundary condition for the plate at the shoulder/ plate interface; and q_2 - the heat flux boundary condition at the probe/plate interface.

Expressions for q_1 and q_2 are similar and are calculated according to:

$$k\frac{\partial T}{\partial n}=q \tag{6}$$

Welding parameters and dimensions of the welding tool used for the numerical simulation of the FSW process are: v_{wel} = 1.59 mm/s; v_{rot} = 500 rpm; h_A = 12.25 W/m^{2}K; h_b = 6.25 W/m^{2}K; $T_{Al\text{-}melting}$ = 933 K; r_{probe} = 3 mm; $r_{shoulder}$ = 13 mm; h_{probe} = 5 mm; k = 160 W/mK; ρ = 2700 kg/m^3 and c = 900 J/kgK. These parameters are the same for both joints.

NUMERICAL RESULTS

Temperature distributions through cross section of the T- and butt joint in the direction of the joint line (x-axis) are shown in Figs. 6 and 7, respectively. As expected, the temperature values are presented in the area immediately around heat sources, i.e. forehead on the top of shoulder and near the probe. In both cases, the thickness of the plates is 6 mm.

The maximum value of temperature that occurs during numerical simulation of the T-joint is 662°C, Fig. 6. Results for the butt joint are shown in Fig. 7, indicating that the maximum temperature is 553°C.

Figure 8 shows the distribution of temperature fields in the T-joint, seen from the side where the plates are in contact with the backing plates.

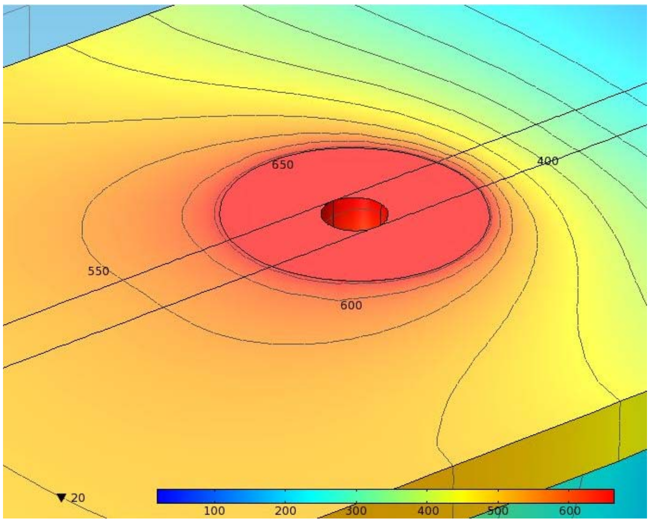

Figure 6. Temperature fields in the x-y plane, /4/.

Figure 7. Temperature distribution (FEM) study, /4/.

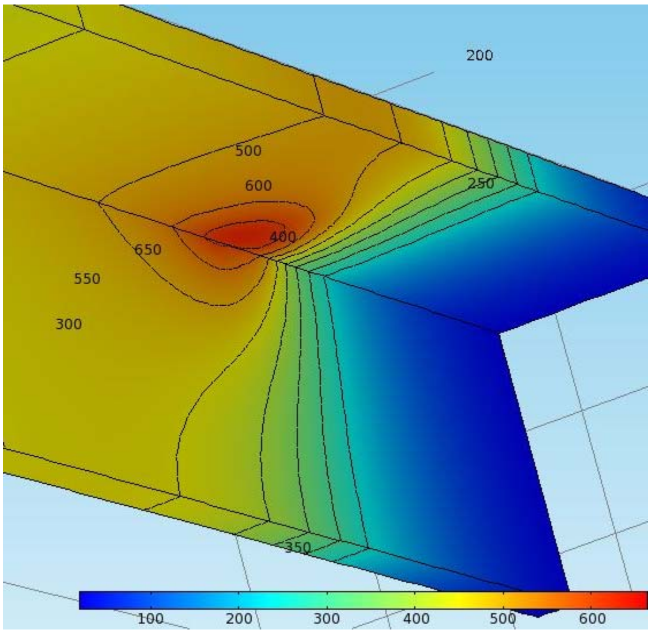

Figure 8. Temperature fields viewed from the side where the plates are in contact with the backing plate, /4/.

DISCUSSION AND CONCLUSION

Nonlinear finite element analysis is performed for a friction stir welding of Al alloys, both for the T- and butt joint. It has been shown that T-joints are not only an extension of a classical butt welding, but also feature some peculiarities in a heat flow and temperature distribution due to the geometrical aspects of the T-joint. Higher value of the temperature is observed in the simulation of the welding of a T-joint. A selection of different welding parameters of the process temperature can be reduced.

Heat input is the most important parameter in FSW, affecting quality of the joint. This effect can be seen clearly in Fig. 9, where two T-joints are presented, one made in a single pass (Fig. 9a) with lower heat input; and the other made with passes (Fig. 9b) of higher heat input. It is clear that the shape of the T-joint is better in the first case, but one can also notice a defect in this case, as a result of a lack of heat input. Contrary to that, the two-pass welded joint has no defects, but its shape is not appropriate due to the excessive heat input.

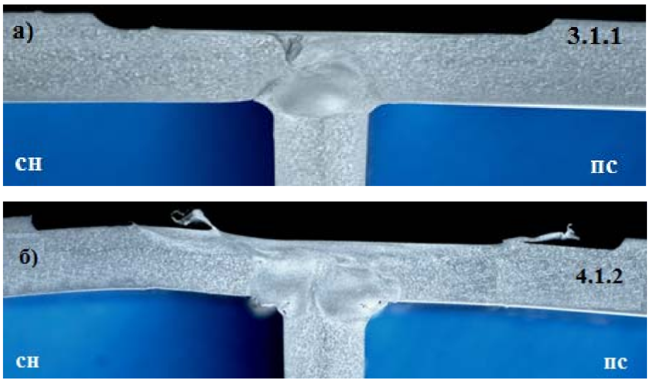

Figure 9. a) single pass weld; b) two-pass weld.

Based on the results and discussion, one can conclude that the numerical simulation can be a powerful tool to estimate the heat effects in FSW, and thus, to predict the quality of the welded joints.

ACKNOWLEDGEMENT

This research is partially supported by the Ministry of Education, Science and Technological Development of the Republic of Serbia through Grant ON 174004.

REFERENCES

1. Shultz, E.F., Cole, E.G., Smith, C.B., et al. (2010). *Effect of compliance and travel angle on friction stir welding with gaps*, J Manuf. Sci. Eng., 132(4): 1-9.
2. Tang, W., Guo, X., McClure, J.C., Murr, L.E., Nunes, A. (1998). *Heat input and temperature distribution in friction stir welding*, J Mater. Proc. and Manuf. Sci., 7(2): 163-172.
3. Colegrove, P., Painter, M., Graham, D., Miller, T., *3-Dimensional flow and thermal modeling of the friction stir welding process*, Proc. of Second Int. Symp. on FSW, Gothenburg, Sweden, June 2000, (distributed by TWI on CD).
4. Đurđević, A., *Friction stir welding technology of aluminium alloy T-joints*, PhD Thesis (in Serbian), University of Belgrade, Faculty of Mechanical Engineering, 2015.
5. Živojinović, D., *Fracture mechanics application on integrity assessment of welded construction made from aluminum alloys*, PhD Thesis (in Serbian), University of Belgrade, Faculty of Mechanical Engineering, 2013.
6. Munoz, A.C., Ruckert, G., Huneau, B., Sauvage, X., Marya, S. (2008), *Comparison of TIG welded and friction stir welded Al-4.5 Mg-0.26Sc alloy*, J Mater. Proc. Tech., 197(1-3): 337-343.
7. https://www.asm.matweb.com
8. https://www.arconic.com/global/en/who-we-are/global-rolled-products.asp
9. Đurđević, A., Sedmak, A., Živković, A., Đurđević, Đ., *Macrostructures, defects and microhardness of friction stir welded T joints of AA 5052 and AA 5754-H111,* 7th Int. Sci. Expert Conf. TEAM 2015, pp.523-527, Belgrade, Serbia (2015).
10. Dong, P., Lu, F., Hong, J.K., *Analysis of weld formation process in FSW*, Proc. 1st Int. Symp. on FSW, Thousand Oaks, California, USA (1999).
11. Peel, M.J., Steuwer, A., Withers, P.J., Dickerson, T., Shi, Q., Shercliff, H. (2006). *Dissimilar friction stir welds in AA5083-AA6082 Part I: Process parameter effects on thermal history and weld properties*, Metall. and Mat. Trans. A, 37(7): 2183-2193.
12. Cao, X., Jahazi, M. (2011). *Effect of tool rotational speed and probe length on lap joint quality of a friction stir welded magnesium alloy*, Mat. and Design, 32(1): 1-11.